Supporting information

Switchable dual-band generation of femtosecond pulses in a mode-locked Erbium-doped fiber laser based on monolayer graphene

Sergio Castrillon. S.[1,2] , Esteban M. A.[1,3] , David Steinberg[2] , Andrés B. Pérez[4] , Javier F. Botia[1], Ana M. Cardenas[1] , Lucia A. M. Saito[2] , EA Thoroh de Souza[2] and Juan D. Zapata[1,*]

[1]Applied Telecommunications Research Group (GITA), Faculty of Engineering, Department of Electronic Engineering, Universidad de Antioquia (UdeA), Calle 50 No. 73–21, 050034, Medellín, Colombia.

[2] Mackenzie Presbyterian University, School of Engineering, Rua da Consolação, 930–São Paulo/SP, 01302-907, Brazil.

[3]Grupo de Optica y Fotonica, Instituto de Fisica, Universidad de Antioquia U de A, Calle 70 No. 52-21, Medellin, Colombia.

[4]Departamento de Electrónica y Telecomunicaciones, Instituto Tecnológico Metropolitano (ITM), Medellín 050012, Colombia

Experiments were carried out by one week period using the same initial conditions. The main goal was to study the pulse generation by linearly varying the pumping power (PP).

Experiment 1 yielded four polarization states as identified by four mode-locking (ML) regions: single band ML at 1530 and 1556 nm, stable and unstable dual-band, configurations. After one week, the Experiment 2 was conducted to reproduce the same previous ML regions: single band at 1530 nm, stable and unstable dual-band configurations, and a switchable mode-locking state from 1530 to 1556 nm.

Section 1 : Spectra as a function of pumping power

Mode locking 1530-nm GB

Data experimental 1 ---------- Data experimental 2

Decreasing PP

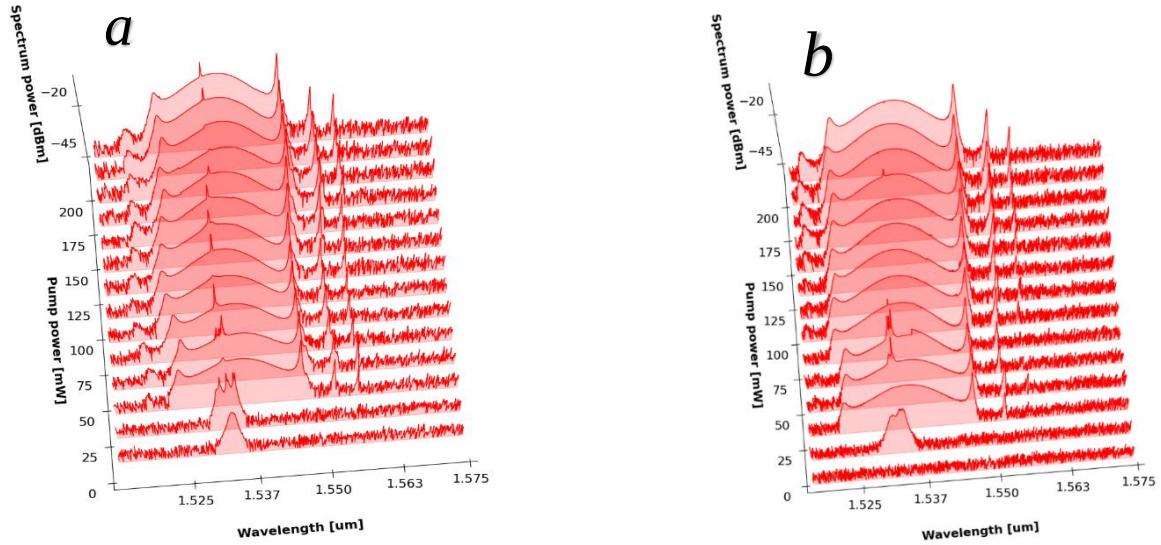

Increasing PP

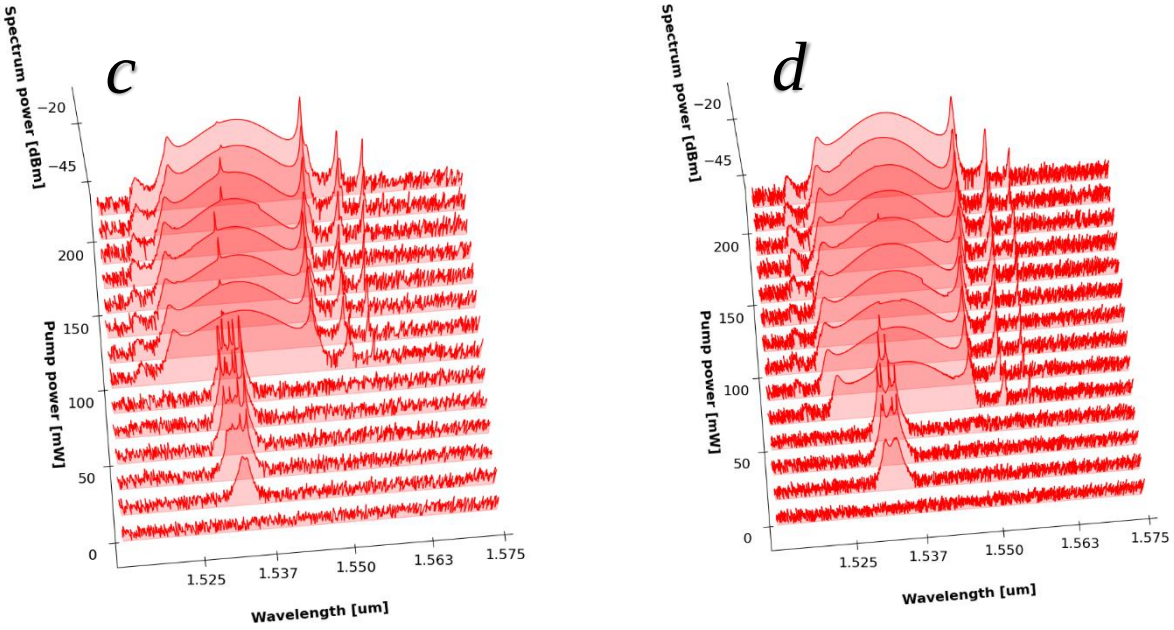

Figure S1. Spectral evolution of mode locked in 1530 nm GB as a function of PP for two different experiments. Top side correspond to a decreasing the PP, a) experiment 1, b) experiment 2. Bottom side correspond to an increasing the PP, c) experiment 1 and d) experiment 2.

Mode locking 1556-nm GB

Data experimental 1 ---------- Data experimental 2

Decreasing PP

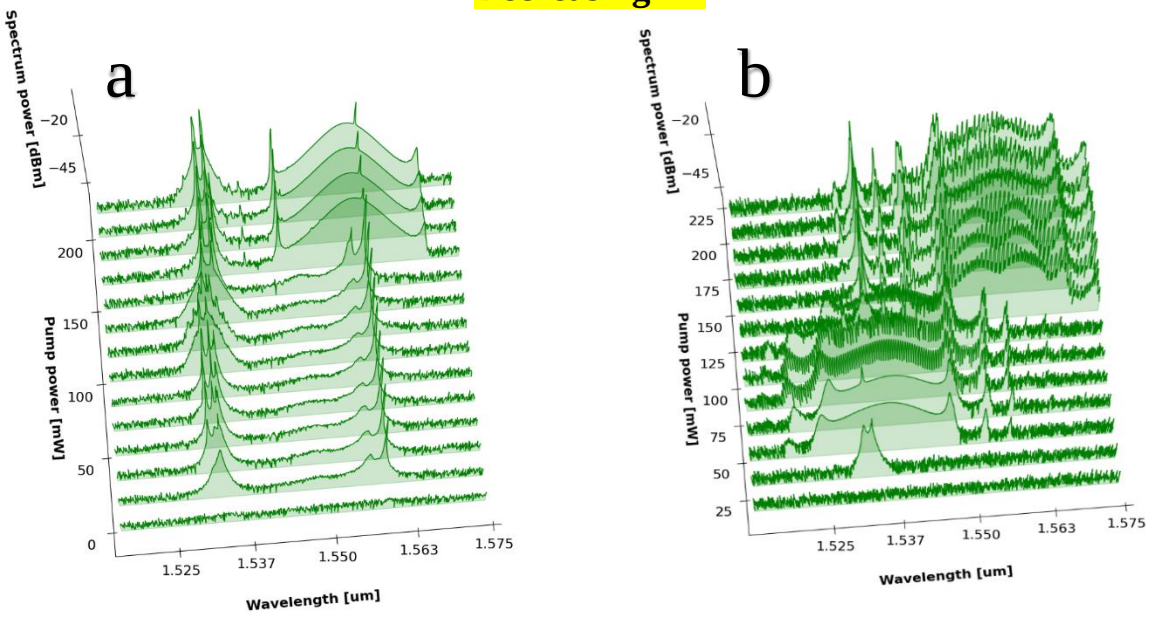

Increasing PP

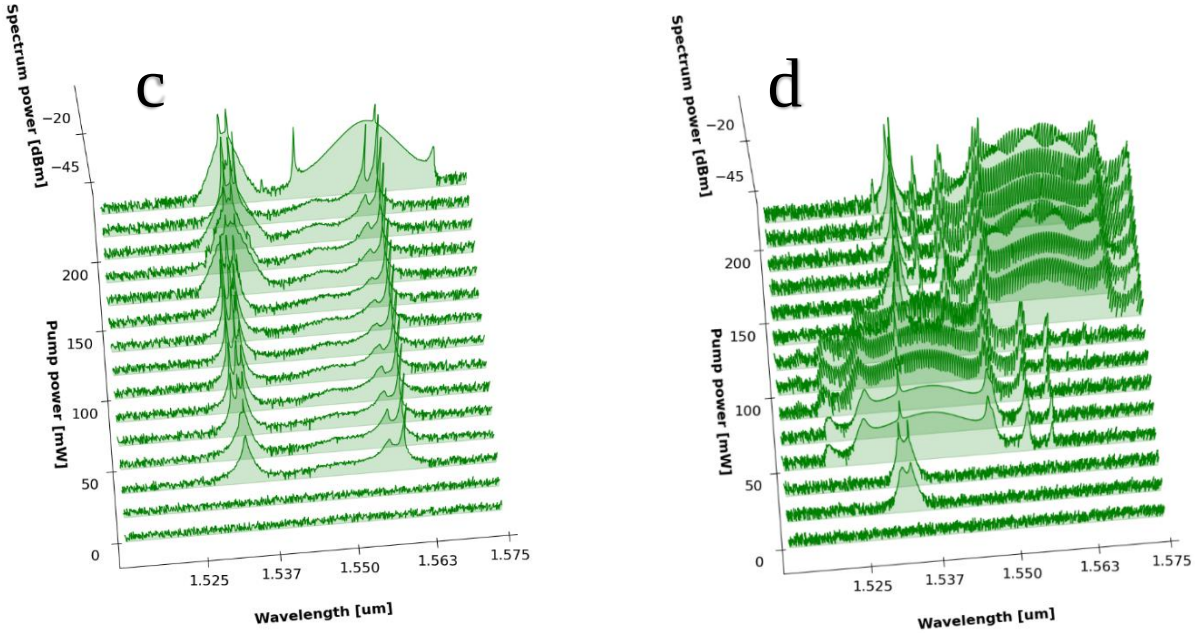

Figure S2. Spectral evolution of mode mocked in 1556 nm GB as a function of PP for two different experiments. Top side correspond to a decreasing the PP, a) experiment 1, b) experiment 2. Bottom side correspond to an increasing the PP, c) experiment 1 and d) experiment 2.

Instable DB configuration

Data experimental 1 ----------Data experimental 2

Decreasing PP

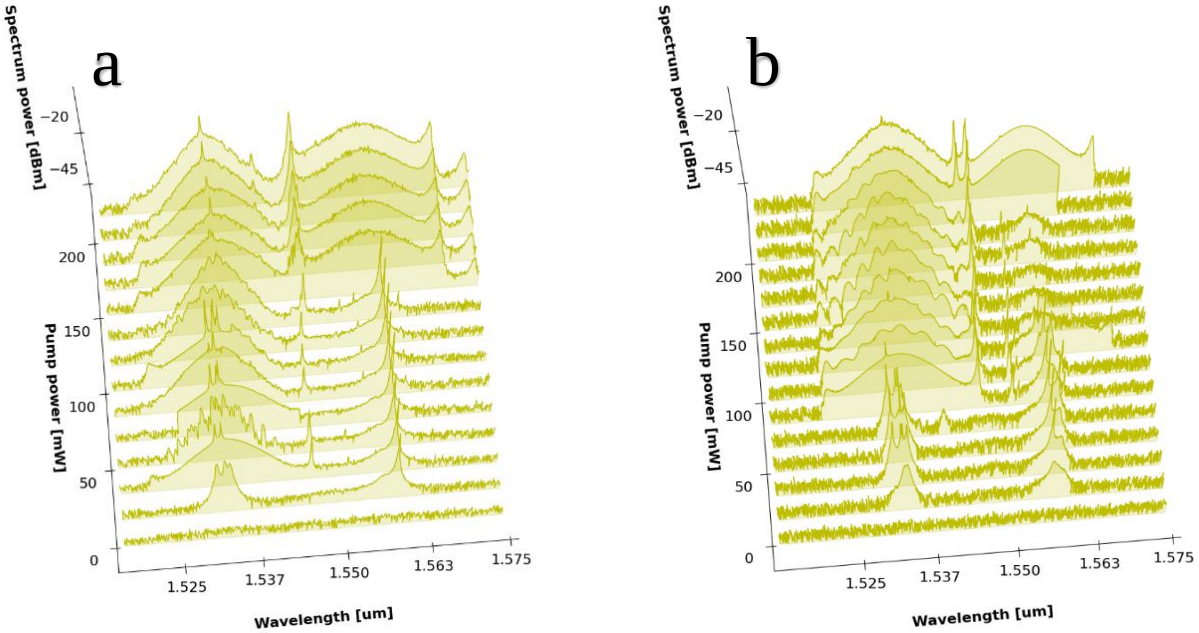

Increasing PP

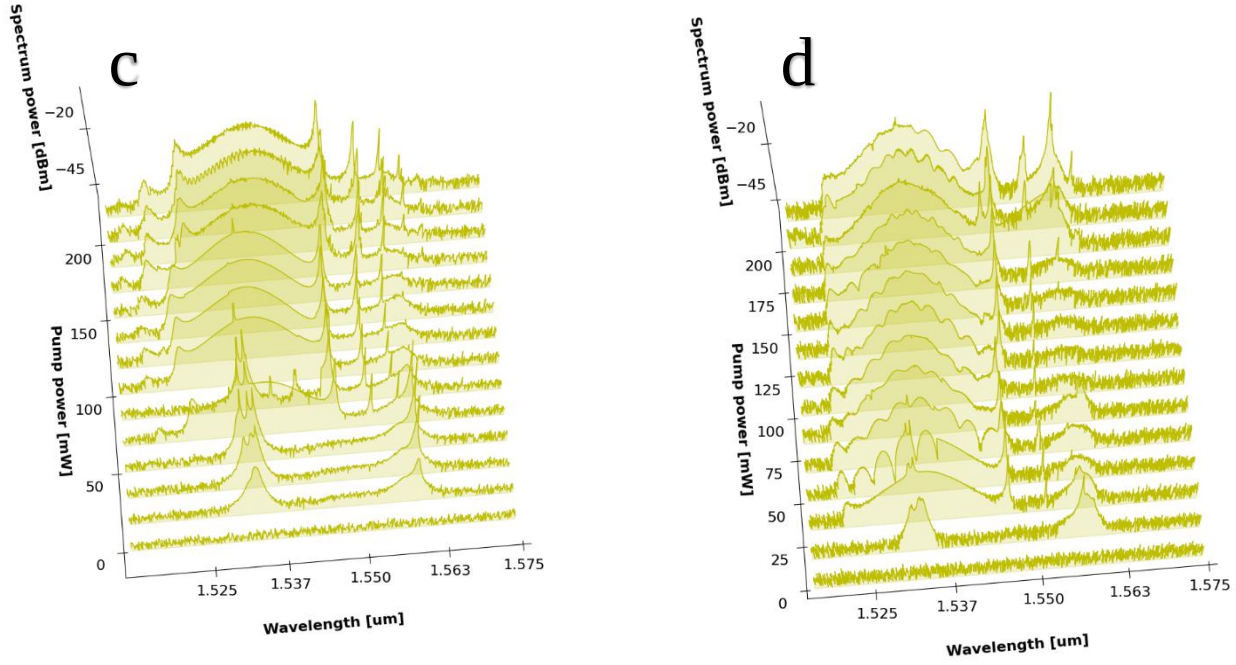

Figure S3. Spectral evolution of instable DB configuration as a function of PP for two different experiments. Top side correspond to a decreasing the PP, a) experiment 1, b) experiment 2. Bottom side correspond to an increasing the PP, c) experiment 1 and d) experiment 2.

Stable DB configuration.

Data experimental 1 ---------- Data experimental 2

Decreasing PP

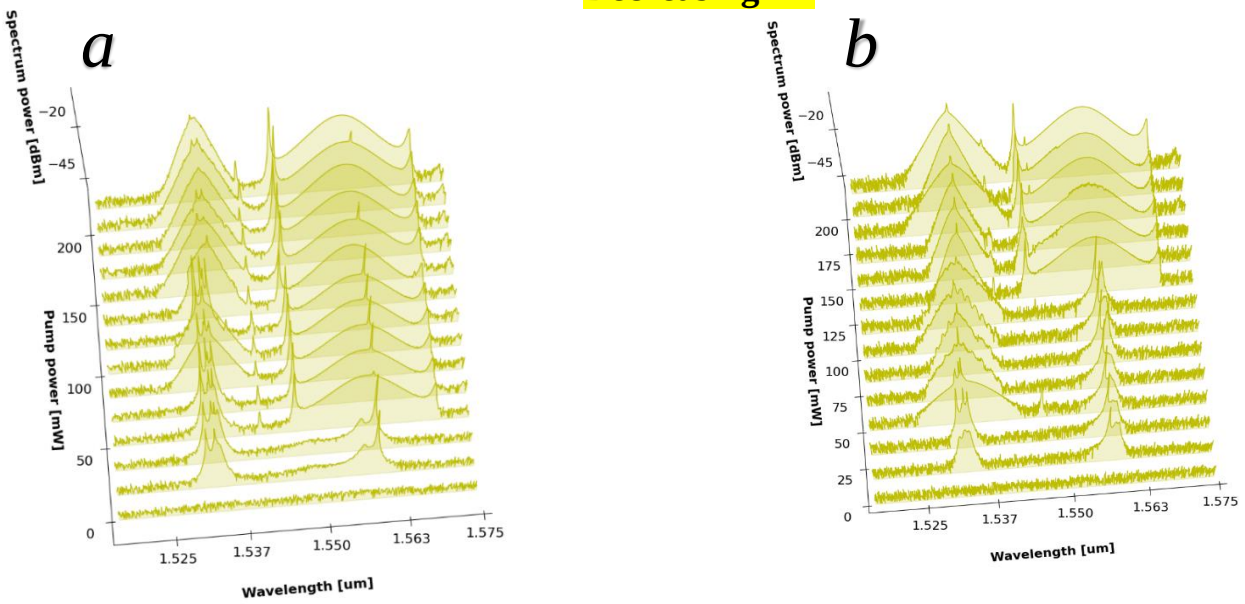

Increasing PP

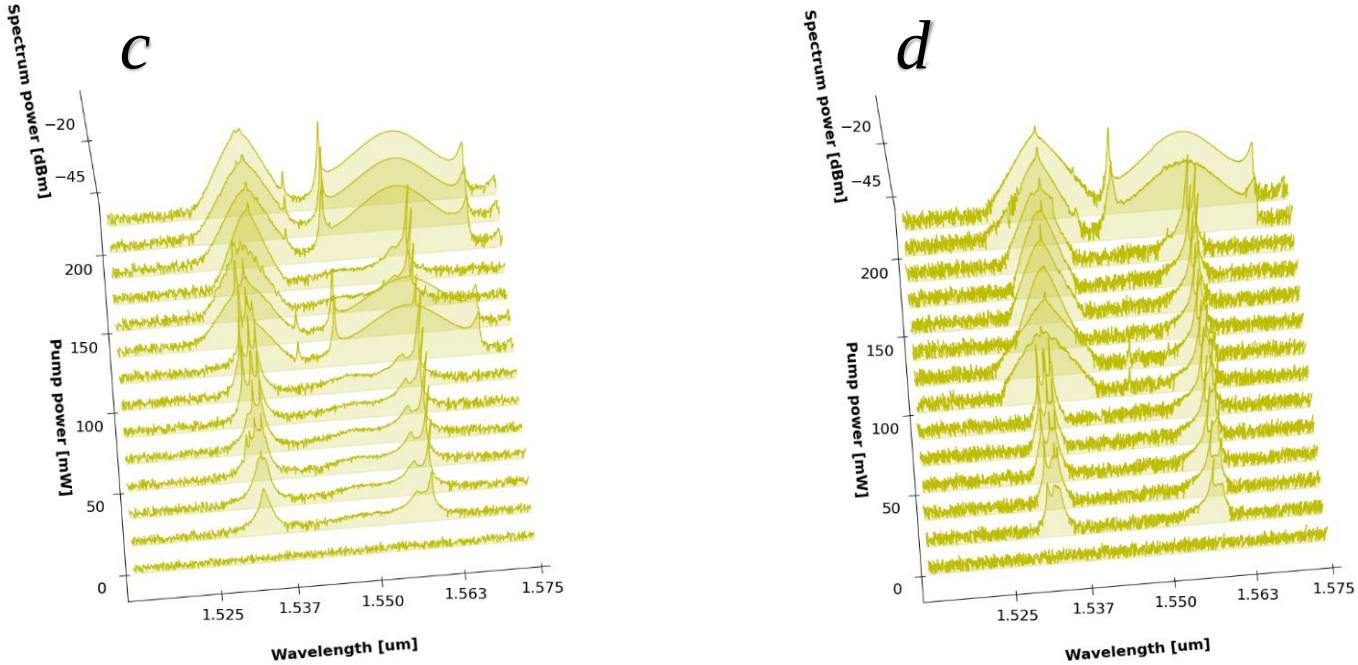

Figure S4. Spectral evolution of stable DB configuration as a function of PP for two different experiments. Top side correspond to a decreasing the PP, a) experiment 1, b) experiment 2. Bottom side correspond to an increasing the PP, c) experiment 1 and d) experiment 2.

In all results, we observed that the mode-locking regime was maintained at lower PP after obtaining the pulse and starting to decrease the PP, while when restarting the pumping power from 0 mW, a higher value was required. On the other hand, the unstable double-band configuration showed spectra with greater widening, but these tended to lose their stability and were no longer in mode-locking regime, while stable dual bands maintained their stability at different PP. Finally, the single band mode-locking at 1556 nm GB exhibited an interesting switchable state as function of PP.

Section 2: Variation of parameters in a simulation *(Dispersion and Saturable absorber).*

The net intracavity dispersion and laser repetition rate are directly associated with cavity length. One of the advantages of fiber lasers is that they change these parameters without extreme complexity by adding more or less optical fiber spans into the cavity system. The value of the cavity length and the type of fiber were chosen to balance the dispersion and nonlinear effects into the cavity so that solitons could be generated. Additionally, the length of the erbium-doped fiber (EDF) is one of the main parameters regarding the observation of DB regime in EDFLs since different lengths of EDF as a gain medium can lead to variations in the saturation power of the gain medium, for example, thus inducing a significant change of the intracavity power for DB generation. Moreover, the input loss can also increase as a function of a given saturable absorber.

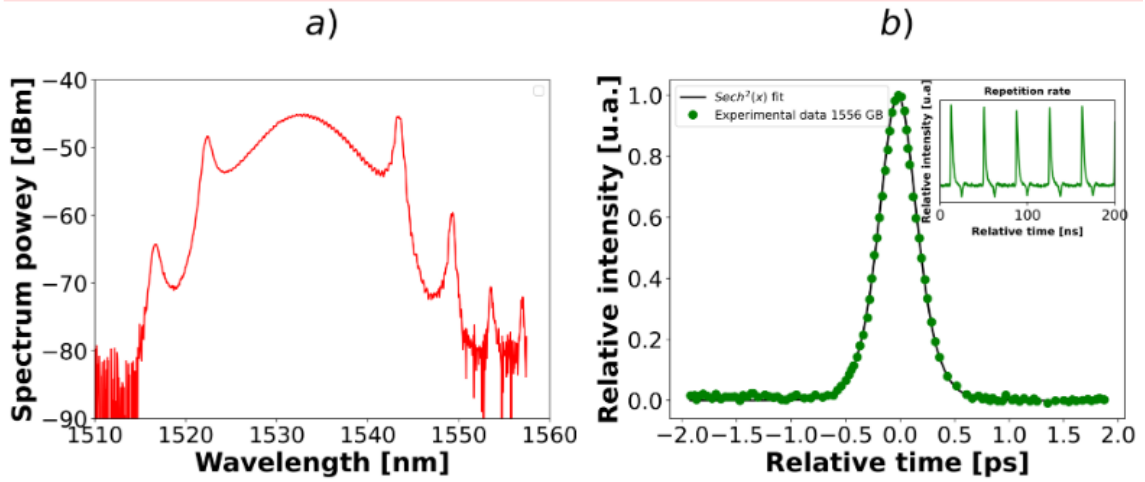

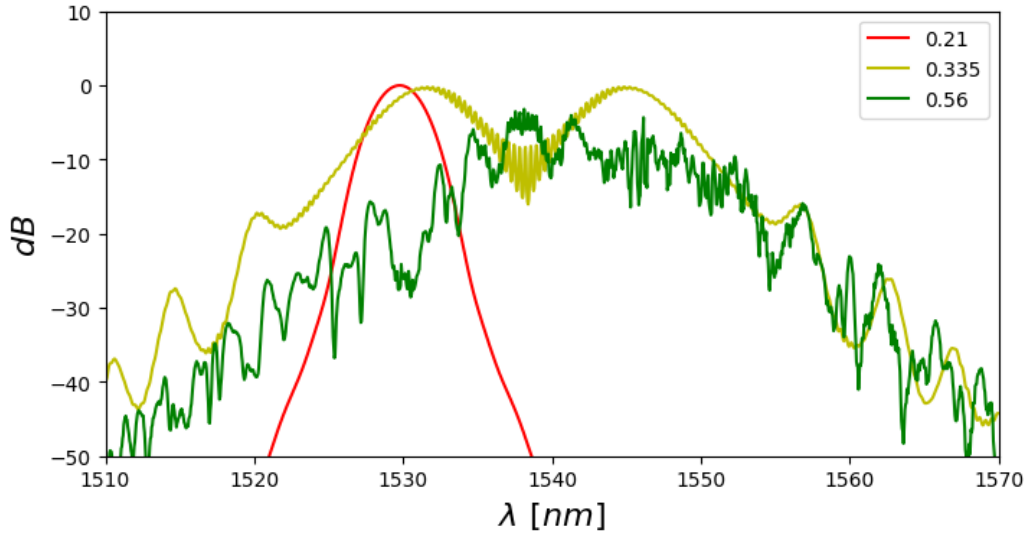

Figure S5: Experimental 1530 nm mode-locked EDFL pulse obtained for 0.21 m gain medium laser cavity. a) Spectrum and b) Autocorrelation pulse with its repetition rate of 26.7 MHz. c) Mode-locking spectrum formation as a function of changing Erbium parameters. Legend's red, yellow, and green curves represent the generated spectrum for each EDF length of 0.21, 0.335, and 0.56 m, respectively. For the same labels, we used saturation power and N of 0.0608 mW (N= 0.7), and 0.965 mW (N=0.63), and 3.4 mW (N=0.55), respectively

On the other hand, the experiment setup was changed too, reducing the EDF length to 20 cm. Fig. S5a shows the spectrum associated with a new laser cavity, centered to 1533 nm, with a spectral width of 3 dB around 9.4 nm and Fig. S5b shows a temporal measure of pulse with a pulse duration of around 389 fs and a new repetition rate of 26.7 MHz.

Moreover, we analyzed the DB generation using two other 2D nanomaterials, molybdenum disulfide (MoS2) and black phosphorus (BP) as saturable absorbers (both reported in literature) at our laser configuration to compared with graphene (Fig. S6). For each material, we fixed all laser parameters to achieve the dual band presented in the paper and changed only the saturable absorber parameters according to Table 1. The simulation results revealed the generation of DB as promoted only by graphene given the parameters of our cavity, such as dispersion, gain medium length, etc. This may be due to the ability of modulating the intracavity intensity to values at which the erbium gain spectrum allows laser operation at a specific wavelength and its polarization extinction ratio. However, under a series of optimized simulation parameters, it may be possible to find the switchable behavior via the change of gain medium, dispersion and cavity loss parameters.

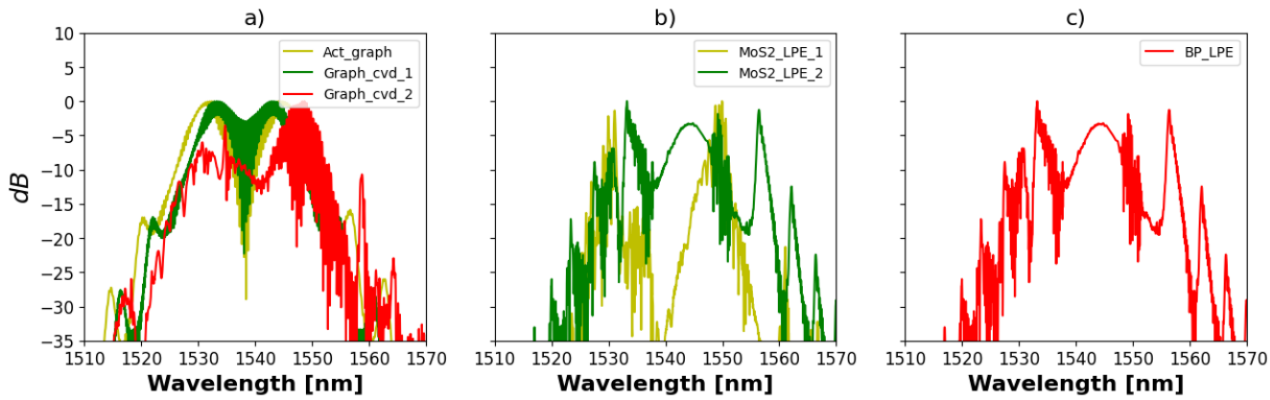

Figure S6 : Dual-band (DB) simulation in EDFL using different saturable absorber parameters. a) graphene (actual – yellow curve; ref. 1 – green curve; ref. 2 – red curve). b) MoS2_(ref. 3 – yellow curve; ref. 4 – green curve) and c) BP (ref. 5 – red curve). See specific information in Table 1.

Fig. S6 presents simulation results for different saturable absorbers reported in the literature. We fix all the parameters necessary for getting the Dual band and change the saturable absorber parameters according to Table 1 for each respective material. As expected, the Kelly bands of the formed spectra are shifted.

Nanomaterial	Type	s(%)	Is(MW/cm2)
Graphene	CVD	66.5	0.61
Graphene	CVD	6.2	0.71
MOS2	LPE	4.3	34
MOS2	LPE	1.2	158
BP	LPE	6.91	433

Table 1: Saturation parameters of each nanomaterial. Type represents the fabrication method of nanomaterial. CVD: Chemical vapor deposition. LPE: Liquid phase epitaxy. ME: Mechanically exfoliated.

Section 3: Output power as a function of paddles position.

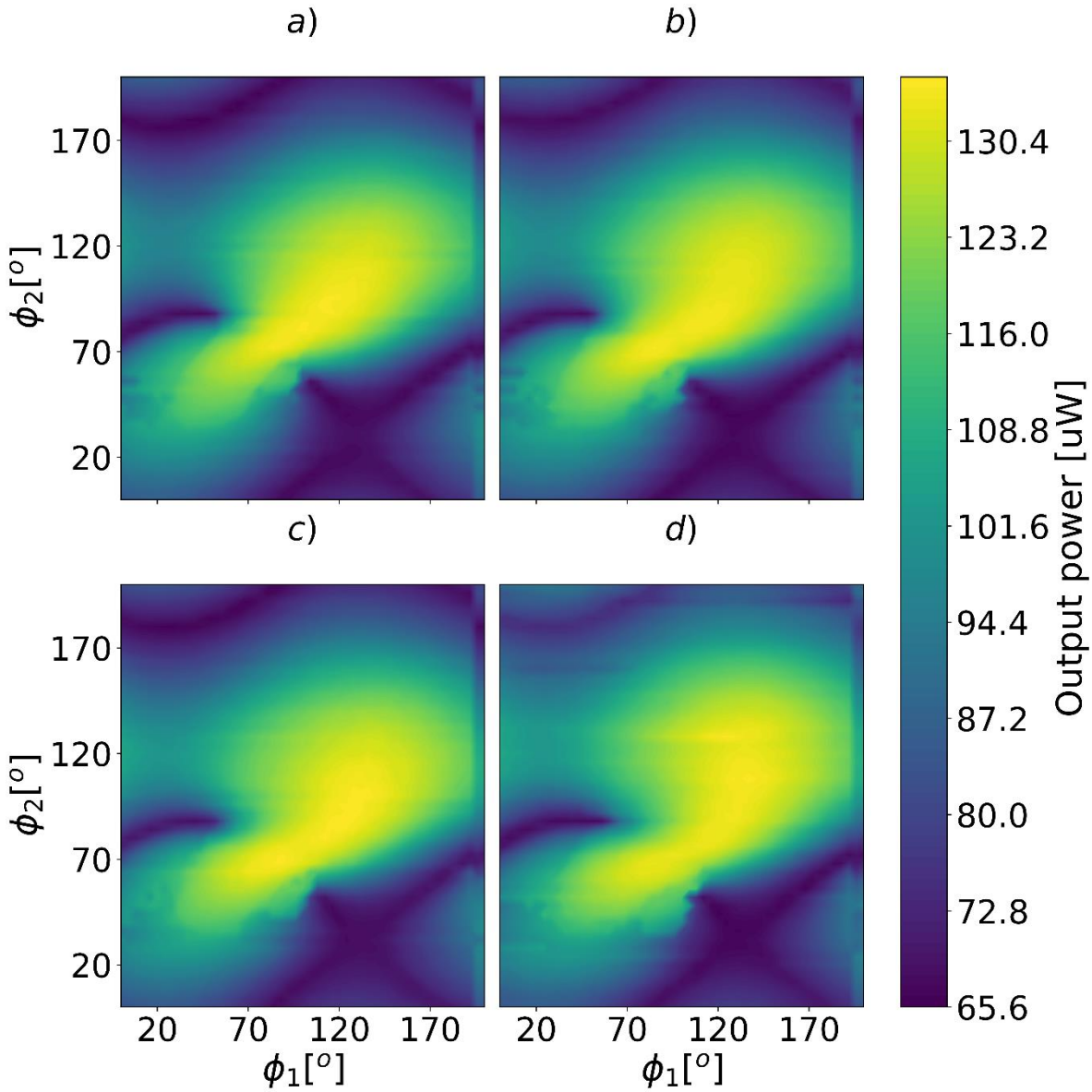

Figure S7: Output power results as a function of polarization state a) φ3 = 16, b) φ3 = 20, c) φ3 = 24 and d) φ3 = 28

This map shows, like the classes, a certain synchrony for small perturbations, which seems to confirm the stability of the system to repeated measurements at long exposure times. However, know other variables of the system such as polarization for a better understanding.

REFERENCES

1. Qiming Zhao, Shouyan Zhang, Shuxian Wang, Gang Wang, Haohai Yu, Huaijin Zhang, Saturable absorption and visible pulse modulation of few-layer topological nodal-line semimetal HfGeTe, Chinese Optics Letters, 10.3788/COL202422.031601, 22, 3, (031601), (2024).

2. H. Zhang, D. Y. Tang, L. M. Zhao, Q. L. Bao, and K. P. Loh, "Large energy mode locking of an erbium-doped fiber laser with atomic layer graphene," Opt. Express 17, 17630-17635 (2009).

3. Hao Liu, Ai-Ping Luo, Fu-Zao Wang, Rui Tang, Meng Liu, Zhi-Chao Luo, Wen-Cheng Xu, Chu-Jun Zhao, and Han Zhang, "Femtosecond pulse erbium-doped fiber laser by a few-layer MoS2 saturable absorber," Opt. Lett. 39, 4591-4594 (2014).

4. Yadong Wang, Dong Mao, Xuetao Gan, Lei Han, Chaojie Ma, Teli Xi, Yi Zhang, Wuyun Shang, Shijia Hua, and Jianlin Zhao, "Harmonic mode locking of bound-state solitons fiber laser based on MoS2 saturable absorber," Opt. Express 23, 205-210 (2015).

5. Yu Chen, Guobao Jiang, Shuqing Chen, Zhinan Guo, Xuefeng Yu, Chujun Zhao, Han Zhang, Qiaoliang Bao, Shuangchun Wen, Dingyuan Tang, and Dianyuan Fan, "Mechanically exfoliated black phosphorus as a new saturable absorber for both Q-switching and Mode-locking laser operation," Opt. Express 23, 12823-12833 (2015).